RADIATION PROTECTION ASPECTS AT THE ELECTRON RECOVERY AREA OF THE ELI-NP GAMMA BEAM SYSTEM

Maria-Ana POPOVICI[1], Iani-Octavian MITU [2], Gh. CATA-DANIL[3]

The ELI-NP Gamma Beam System will provide a very intense and brilliant gamma beam which is obtained by incoherent Compton back-scattering of direct laser light with a very intense electron beam. The electrons are subsequently dumped in the electron recovery area (ERA) of the ELI-NP experimental building. In this paper we discuss some radiation protection aspects imposed by the high intensity, low emittance, relativistic electron beam at a repetition rate of 100 Hz. A beam dump system and local shielding are proposed in order to comply with assumed dose constraints outside the building ($0.1\ \mu Sv/h$). Both simplified calculations and FLUKA simulation results were used to motivate the material and geometry selection. The radial and longitudinal display of the beam dump were optimized for maximum effectiveness. Ambient dose equivalent rate maps throughout ERA and adjacent zones are represented and fluence rate maps of the main secondaries are discussed.

Keywords: Electron beamdump, electron recovery area, FLUKA, total ambient dose equivalent rate

1. Introduction

The electron recovery area (ERA) of the Gamma Beam System (GBS) at ELI-NP represents a challenge from a radioprotection point of view due to the characteristics of the beam that needs to be stopped and the relative proximity of the public area, where the assumed dose constraints are very low ($0.1\ \mu Sv/h$). The electron beam will be provided by a high brightness normal conducting linac accelerator operating at a repetition rate of 100 Hz [1]. For shielding reasons a beam absorber has to be placed in the recovery area. This paper presents a beam

[1] Lecturer , Physics Dept., University POLITEHNICA of Bucharest, Romania, email: popovici@physics.pub.ro
[2] Post Doctoral Research Assistant, ELI-NP, Bucharest, Romania, email: iani.mitu@eli-np.ro
[3] Prof., Physics Dept., University POLITEHNICA of Bucharest, Romania, email: cata-danil@physics.pub.ro

dump system and local shielding proposal based on FLUKA Monte Carlo code simulations.

2. Electron source term and simulation setup

In the present study we took into consideration an electron beam with narrow Gaussian energy distribution ($E_{\text{ave}} = 0.72$ GeV and $\text{FWHM} = 3.6 \cdot 10^{-4}$ GeV) and small divergence (0.05 mrad). The charge per pulse was $Q_{\text{ave}} = 16$ nC/pulse at a frequency $f = 100$ pulse/sec. Thus, the beam dump system was designed for a current $I_{\text{ave}} = Q_{\text{ave}} f = 1.6 \cdot 10^{-8}\,\text{C/pulse} \cdot 100\,\text{pulse/sec} = 1.6 \cdot 10^{-6}\,\text{A}$. The average power that has to be absorbed by the beam dump is $P_{\text{ave}} = \left(I_{\text{ave}}/e\right) E_{\text{ave}} = 1.152 \cdot 10^{3}\,\text{W}$, with a number of electrons per pulse $N_{\text{e}^-}^{\text{pulse}} = Q_{\text{ave}}/e = 1.0 \cdot 10^{11}\,\text{e}^-/\text{pulse}$, which leads to an average energy per pulse $E_{\text{ave}}^{\text{pulse}} = N_{\text{e}^-}^{\text{pulse}} \cdot E_{\text{ave}} = 11.52\,\text{J/pulse}$.

The present FLUKA simulations were carried out with FLUKA 2011.2c.0 and Flair 2.0-5 [2, 3, 4]. To improve the statistics in sampling photonuclear reactions, the inelastic interaction length of photons was reduced 50 times. Also, the geometry of the concrete cage and walls was subdivided into more regions and importance biasing was applied to compensate for attenuation and maintain a fairly constant population throughout the geometry. This allows for estimates of dose outside the bulk shielding, where the strictest constraints are imposed.

3. Characterization of the electromagnetic cascades for beam dump materials selection

The primary electrons interact with the dump material and, due to their high energy (0.72 GeV), give rise to electromagnetic cascades. The processes by which they lose energy are mainly ionization and excitation of the dump material atoms (collision losses) and radiation losses (bremsstrahlung). In this case, for the highly relativistic electrons ($\gamma = 1.44 \cdot 10^{3}$), collision energy loss is approximately constant, and the radiation loss increases approximately linearly with the primary energy. The characteristic distance in a material over which the electron energy decreases in average e times with respect to the initial value is the radiation length, X_0, which can be estimated by using an approximate equation [5]

$$X_0 = \frac{716\ \text{g/cm}^2 \cdot A}{Z(Z+1)\cdot \ln\left(287/\sqrt{Z}\right)} \cdot \frac{1}{\rho}\ , \tag{1}$$

where A and Z are the mass and atomic, respectively, numbers and ρ is the mass density expressed in g/cm^3. The limit value of the energy for which the two mechanisms of energy loss contribute equally is called the critical energy, E_c and, for solids and liquids, it can be estimated by an approximate equation [5]:

$$E_\text{c} = \frac{610\ \text{MeV}}{Z+1.24}\ . \tag{2}$$

The development of the shower in the longitudinal direction can be described by a parameter which gives the length of a homogeneous cylinder, extending infinitely in the radial direction, over which 99% of the primary energy is absorbed, $L_{99\%}$. It can be estimated as a function of the initial energy (in our case E_ave), the critical energy E_c - both expressed in MeV, and the radiation length X_0, in cm [6]:

$$L_{99\%} = \left(1.52\ln\left(\frac{E_\text{ave}}{\text{MeV}}\right) - 4.1\ln\left(\frac{E_\text{c}}{\text{MeV}}\right) + 17.6\right) X_0\ . \tag{3}$$

The radial development of the electromagnetic shower is described by a parameter called the Moliere radius, R_M, which can be estimated as a function of the critical energy, in MeV and radiation length, in cm by an approximate equation [6]:

$$R_\text{M} = \frac{21.2\ \text{MeV}}{E_\text{c}} X_0\ . \tag{4}$$

It can be demonstrated [6] that the radial distance over which a homogeneous, infinitely long cylinder absorbs 99% of the initial electron energy is given by

$$R_{99\%} = 5 \cdot R_\text{M}\ . \tag{5}$$

In our study we considered as possible dump materials: graphite (C), concrete, aluminum, iron and copper. In table 1 we present the values of the density ρ, the specific heat capacity c, the radiation length X_0, the critical

energy E_c, the Moliere radius R_M, the length over which 99% of the initial electron is absorbed, $L_{99\%}$, and the corresponding radial distance, $R_{99\%}$.

Table 1.

Material constants and parameters describing the electromagnetic cascade in the materials selected for beam dump construction

	C	Concrete	Al	Iron	Cu
$\rho\left(\mathrm{g/cm^3}\right)$	1.71	2.30	2.70	7.87	8.96
$c\left(\mathrm{J/g\cdot K}\right)$	0.71	0.96	0.91	0.45	0.39
$X_0\left(\mathrm{cm}\right)$	19.32	11.55	8.897	1.757	1.436
$E_c\left(\mathrm{MeV}\right)$	81.74	49.9	42.70	21.68	19.42
$R_M\left(\mathrm{cm}\right)$	5.012	4.909	4.419	1.719	1.568
$L_{99\%}$ (cm)	184.4	133.6	108.6	26.3	22.2
$R_{99\%}$ (cm)	25.1	24.5	22.1	8.6	7.8

Wide experience existing at electron accelerators showed that an effective and stable (from a thermal and mechanic point of view) beam absorber should be composed of a core made of a relatively low Z material surrounded by one or more shells of high thermal conductivity, with small Moliere radius, and a back stop, made of one or relatively high Z materials with good attenuation properties. The low Z core has the role to allow the primary energy to be absorbed over a longer distance, producing a relatively small longitudinal power density. Thus the temperature in the beam line direction experiences a smaller local increase. If the increase in temperature is very steep (as it happens when the beam is stopped directly in a metal, for example) the extraction of heat in the radial direction may not suffice to protect the dump from heat damage. A very good candidate for the core is graphite. Another one could be concrete. Graphite is characterized by a low power density in the longitudinal direction, a low neutron production, meaning it does not activate easily, and a relatively large operating temperature (which can be increased by replacing ambient air with some inert gas to impede

the oxidation processes which change the properties of graphite with increasing temperature). Moreover, nowadays special types of graphite are produced, with larger mass density and thermal conductivity close to that of copper. In our calculations we considered an ordinary graphite core 56 cm in diameter and 90 cm length.

Sometimes (and this was the case here) a central hole in the beam line direction is provided and this moves in a controlled way the hot spot of interaction inside the dump core, so that less radiation is back scattered. In our case, the beam line was taken inside the graphite core over a distance of 30 cm. The outer shell that we chose is a copper one (10 cm thick), due to a high thermal conductivity, relatively high density and a small Moliere radius. The dump is placed in a casing of iron (5 cm thick laterally, 15 cm at the back). The backstop was in copper (25 cm thick). An outer borated polyethylene shell was used to moderate and absorb neutrons produced inside the dump**.**

4. Results

In Figure 1 the graph representation of ERA and the adjacent zones is given in a horizontal projection (a) and a vertical projection (b). One can see that the beam absorber was placed inside a concrete cage. This was necessary because the radiation produced by the intense electron beam at a high repetition rate needs to be stopped before it get in the public area. The concrete cage was a solution which was also adopted for the design of the MYRRHA proton beam line [7]. Based on FLUKA simulations, we found that the highest doses were produced over a

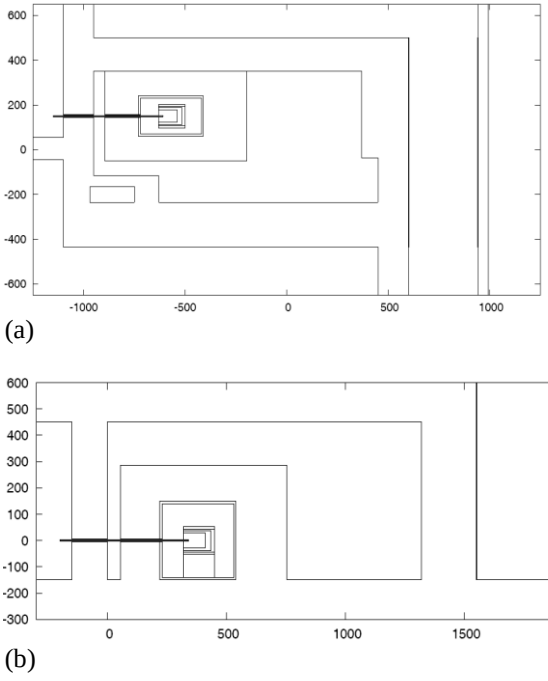

Fig. 1. Geometrical layout of ERA and adjacent zones: (a) horizontal projection; (b) vertical projection

well delimited area, in the forward direction. This is why we placed a 50 cm thick local shielding screen, made of ordinary concrete in the proximity of the South corridor. In the corridor 3 cm-thick wooden panels were used, because wood is an effective low Z neutron shielding material. The outer wall was modeled in gypsum.

FLUKA was used to calculate ambient dose equivalent rates in ERA and adjacent areas. The corresponding map representations of the values expressed in μSv/h can be examined in Figure 2(a) and (b). One can see that, with all the local shielding, the condition that the dose rate outside the building, in the public area, is less that 0.1 μSv/h is fulfilled. The shielding of the neighboring areas is however still not sufficient. Dose rate values in the adjacent laboratory (upper side of Figure 2(a)) are unacceptable ($\geq$ 10 μSv/h) and this requires supplementary local shielding on the other side of the wall over a limited area. The situation in the E7 experimental area is slightly better, but still additional local is recommended since dose rates above 1 μSv/h are obtained.

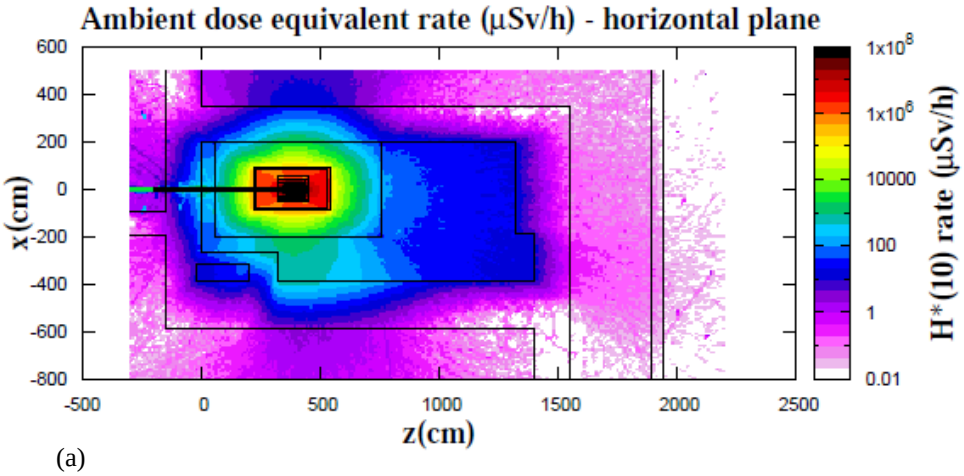

(a)

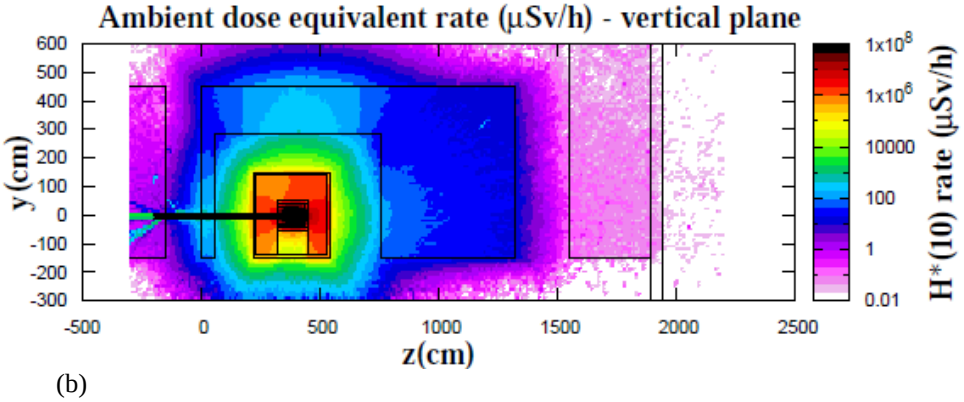

(b)

Fig. 2. All particle dose equivalent rate $H^*(10)$ in $(\mu Sv/h)$ given by the intense electron beam in a 20cm x 20cm cross section sampling volume centered on the beamline: (a) horizontal projection; (b) vertical projection. A number of $1.\times10^{11}$ electrons/ pulse was considered at a pulse repetition rate of 100 Hz.

In Figure 3 the results of the calculations for the secondary radiations are presented. Particle fluence rates expressed in number/cm^2/sec were mapped over the horizontal and vertical projections, in a sampling volume whose cross dimensions are 20cm x 20cm. It can be seen that the complex radiation field produced by this very intense electron beam at high frequency is mainly composed of neutrons and photons. This is understandable if consider that breaking radiation has an energetic spectrum which spans the range from 0 to 720 MeV, and all channels of photonuclear reactions are open. The electrons accounted for in Figure 3(a) and 3(b) along with secondary positrons include the

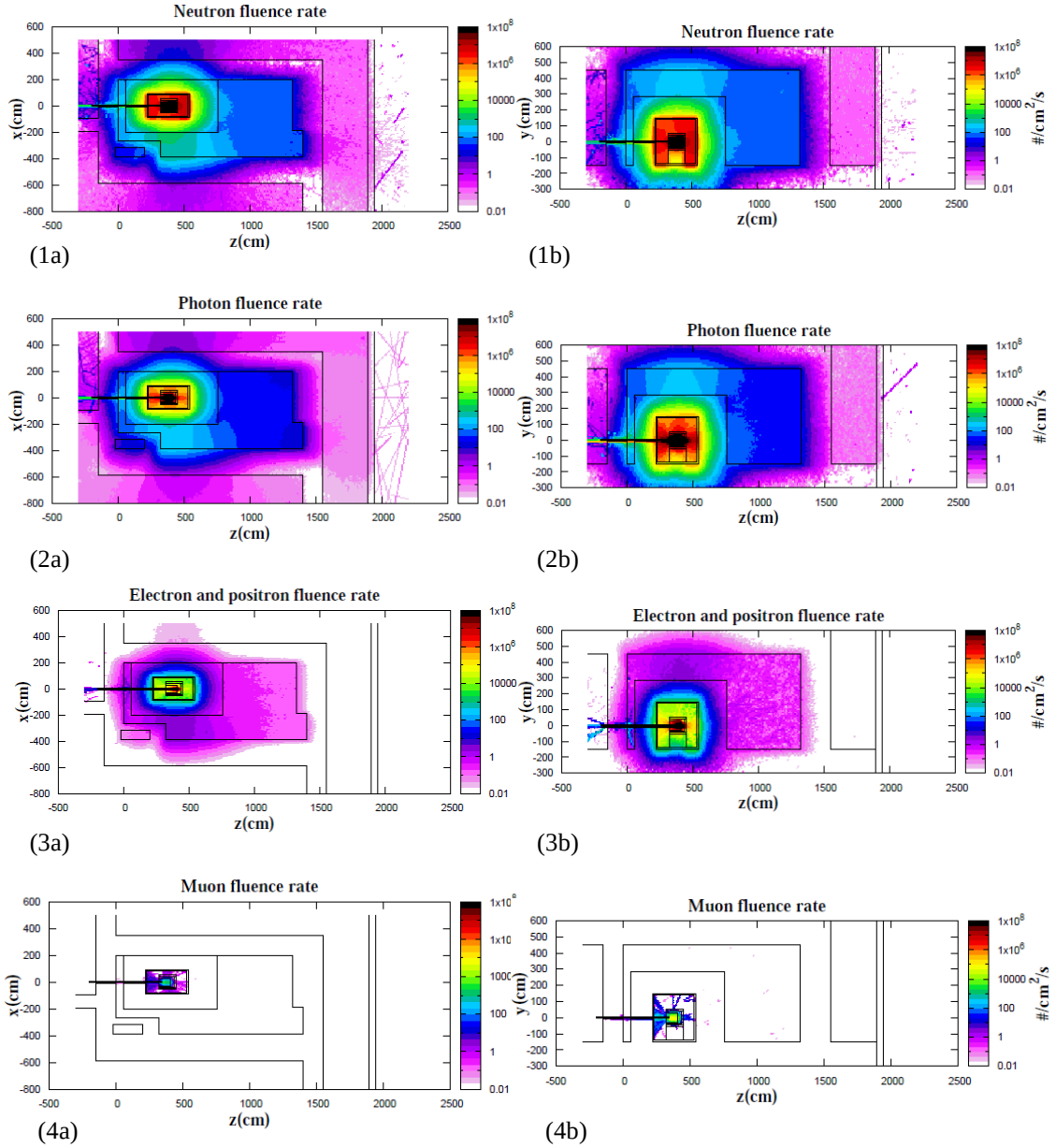

Fig. 3. Particle fluence rate (#/cm^2/s) generated by the intense electron beam in a 20cm x 20cm cross section sampling volume centered on the beamline: (a) horizontal projection; (b) vertical projection: (1a), (1b) neutrons; (2a), (2b) photons; (3a), (3b) electrons and positrons; (4a), (4b) muons. A number of $1.\times10^{11}$ electrons/ pulse was considered at a pulse repetition rate of 100 Hz.

primary radiation. The muons clearly do not represent a problem at this experimental area.

5. Conclusions

The electron recovery area of the Gamma Beam System is a challenge from a radiation protection point of view. In this shielding study we present a beam dump system proposal (absorber plus concrete cage) and local shielding necessary in order to comply with the very low dose constraint (≤ 0.1 μSv/h **)** in the public area. FLUKA simulations used a realistic geometry, according to the project drawing. The beam dump materials were selected by using characteristic quantities for the development of the electromagnetic cascades produced by the intense electron beam in the absorber. Finally, a composite dump with a graphite core and metallic outer shells and backstop was adopted. FLUKA was used to calculate ambient dose equivalent rates over ERA. Secondary radiation fluence rate values were retrieved from the simulation, in order to assess the components which have the most significant contribution to the complex radiation field at ERA. Although the dose constraint in the public area is fulfilled, additional local shielding has to be considered in other adjacent zones.

Acknowledgement

This work was supported by a grant in the programme: CAPACITIES/RO-CERN, project type: ELI-NP, E/04 HHGDE, project number 04/27.06.2014.

R E F E R E N C E S

[1]. *C.A. Ur, D. Balabanski, Gh. Cata-Danil, S. Gales, I. Morjan, O. Tesileanu, D. Ursescu, I. Ursu, N.V. Zamfir,* New frontiers in nuclear physics research at ELI-NP, Acta Physica Polonica B, vol 46, no. 3, 2015

[2]. *A. Ferrari, P.R. Sala, A. Fasso`, J. Ranft,* FLUKA: a multi-particle transport code" CERN-2005-10, 2005, INFN/TC_05/11, SLAC-R-773

[3]. *T.T. Böhlen, F. Cerutti, M.P.W. Chin, A. Fassò, A. Ferrari, P.G. Ortega, A. Mairani, P.R. Sala, G. Smirnov, V. Vlachoudis,* The FLUKA Code: Developments and Challenges for High Energy and Medical Applications, Nuclear Data Sheets vol. 120, 2014, pp. 211-214

[4]. *V.Vlachoudis,* FLAIR: A Powerful But User Friendly Graphical Interface For FLUKA, Proc. Int. Conf. on Mathematics, Computational Methods & Reactor Physics (M&C 2009), Saratoga Springs, New York, 2009

[5]. Particle Data Group, Particle Physics Booklet, July 1996

[6]. *B. Rossi,* High Energy Particles, Prentice Hall, New-York, 1952

[7]. *A. Ferrari, J.L. Blaritte, L. Perot, H. Saugnac, D VandePlassch*e Shielding and activation studies for the design of the MYRRHA proton beamline, Shielding aspects of Accelerators, Targets and Irradiation Facilities - SATIF-11, Workshop Proceedings, Tsukuba, Japan, 11-13 September, 2012